Journal of Engineering and Sustainable Development
Vol. 23, No.02, March 2019
ISSN 2520-0917
https://doi.org/10.31272/jeasd.23.2.6

EFFECT OF MATRIX CHANNEL GEOMETRY ON THE PERFORMANCE OF THE RECOVERY WHEEL

*Dr. Maathe Abdulwahed Theeb[1], Dr. Fouad Alawan Saleh[2], Duaa Jaleel Mohamed[3]

1) Assistant Prof., Mechanical Engineering Department, University of Mustansiriyah , Baghdad, Iraq.
2) Assistant Prof., Mechanical Engineering Department, University of Mustansiriyah , Baghdad, Iraq.
3) M.Sc.Student Mechanical Engineering Department, University of Mustansiriyah, Baghdad, Iraq.

Abstract: In this study, effect of geometry channel of matrix on the performance of the recovery wheel was experimentally and numerically studied. Two channels geometry of matrix (rhombic and sinusoidal) made of aluminum with diameter (60 cm) and length (5, 10, and 15 cm) of wheel were used. A mathematical model for heat transfer between the air and matrix in recovery wheel is derived and solved numerically by using backward difference, fully explicit discretization in time finite difference method. Computer program was built in MATLAB to solve finite difference equations to find the effectiveness of the recovery wheel, and this model is validated with experimental work. The results showed that, the sensible effectiveness for rhombic and sinusoidal channels was increased with increasing wheel speed, also the increase of wheel thickness will increase the sensible effectiveness. When the wheel thickness increased from (5 to 15 cm), the effectiveness will be increase from (74. 39 to 81.48 %) for rhombic, and (79.16 to 85.89 %) for sinusoidal channel at speed (25 rpm). The sensible effectiveness for the sinusoidal channel is higher than the rhombic channel at any wheel speed and wheel thickness increase.

Keywords: *Recovery Wheel, Sensible Effectiveness, Matrix Channel Geometry, Numerical Simulation.*

تأثيرالشكل الهندسي لقناة الحشوة على اداء العجلة المسترجعه

الخلاصة: في هذه الدراسة تمت دراسة تاثير شكل قناة الحشوة على اداء العجلة المسترجعة عمليا ونظريا . شكلين من القناة هم(rhombic and sinusoidal) مصنوعين من المنيوم مع قطر (0.6m) وطول (5, 10, 15 cm) للعجلة تم استخدامها. تضمنت هذه الدراسة جزئيين نظري و عملي. حيث تمت دراسة شكلين من القناة هم(rhombic and sinusoidal) مصنوعين من المنيوم مع قطر (0.6m) وطول (5, 10, 15 cm) للعجلة. الموديل الرياضي لانتقال الحرارة بين الهواء وحشوة العجلة المسترجعة تم حله بالستخدام MATLAB طريقة الفرقات المحددة.تم بناء برنامج باستخدام لحل لحل المعادلات وايجاد اداء العجلة المسترجعة وتم التحقق من البرنامج من خلال المقارنة مع الجزء العلمي . اوضحت النتائج بان الكفاءة المحسوسة لل sinusoidal تزداد بزيادة سرعة العجلة وانه بزيادة سمك الحشوة يزداد اداء العجلة. عند زيادة سمك العجلة (5 – 15 سم) فأن كفاءة العجلة تزداد بمقدار (74.39 – 81.48 %) لل rhombic و (79.16-85.89) ل sinusoidal لسرعة قناة (25 دورة بالدقيقة) . الكفاءة المحسوسة لل sinusoidal تكون اكبر من rhombic لاي نوع من العجلات المسترجعة في اي سرعه وسمك.

* *Corresponding Authors:* maathe@uomustansiriyah.edu.iq

1. Introduction

A recovery wheel employs as a main part of technologies known as heat recovery ventilations (HRVs) or energy recovery ventilators (ERVs). The benefit of combine the recovery wheel with the (HVAC) system is to improve (IAQ), reduce energy consumption, and downsize (HVAC) system. A recovery wheel as shown in figure (1) is a cylindrical wheel rotates at constant rotational speed and divided in to two section by positioned it in a duct system. The frontal area of the wheel is designed to allow air to pass through it from one side to another [1].

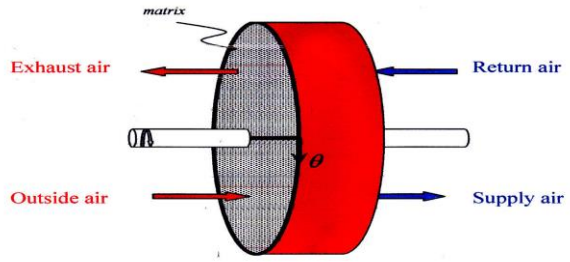

Fig. 1: Recovery Wheel

The heat and moisture in the recovery wheel exchanges in an indirect manner between the supply and exhaust air. When the wheel start to rotate heat is transfer from the hot air to the heat transfer media (matrix) during one half of revolution and from the matrix to the cold air during the second half of revolution. The moisture is transfer in the same manner, during the first half of revolution, the moisture is transfer from the high humid air to the transfer media (matrix) and from the matrix to the low humid air during the second half of revolution [2].

Many investigations have studied the performance of recovery wheel. These studies have investigated the factors that have an influence on recovery wheel performance such as dimension, matrix material, speed of wheel, and the volume flow rate. S. Delfani et al. [3] investigated experimentally and numerically the effect of desiccant wheel length on the sensible and latent effectiveness. Eight different value for the length of wheel at constant diameter were investigated: L=0.1, 0.12, 0.14, 0.16, 0.18, 0.2, 0.22, and 0.24m. It was concluded from the experimental results that the sensible and latent effectiveness rises by increasing the wheel length. Monali S.Bhojane et al. [4] used the energy wheel to improve the performance of C.I engine. Three materials used were mild steel, copper, and aluminum with diameter equal to18 in and thickness 2 in.

They also observed that, aluminum wheel gave the highest performance for all wheel speeds from the other wheels. Manu Prakash et al. [5] studied the energy wheel effectiveness (sensible and latent) at different wheel diameter. The wheel dimension selected for this study is five value of diameter D=500, 600, 700, 800, and 900mm and constant wheel length. It was showed that, when wheel diameter increases both sensible

and latent effectiveness increases because the area of contact increases and the volume flow rate is constant. This study focused on the effect channel geometry of matrix on the performance of the recovery wheel.

2. Theoretical and Numerical Models

The governing deferential equations and finite difference equations will be introduced to estimate the performance of the recovery wheel.The programming and structure of computer codes will be also presented in this section.

2.1 Physical Properties of Recovery Wheel

To form the sensible heat model, it is necessary to illustrate and define the coordinate and nomenclature of the heat wheel as shown in figure (2). The supply side is distinguished by subscript (s) and the exhaust side by (e). The inflow is denoted by (i) while the outflow by (o). the subscripts (m and g) refer to matrix and air flow respectively.

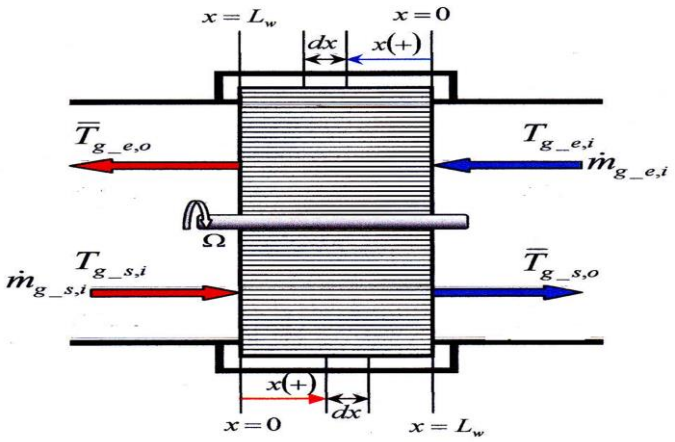

Figure 2. Coordinates and nomenclature of the recovery wheel.

Since the wheel is balanced and symmetric, the wheel frontal area, free flow area, and heat transfer area are the same on each side. They can be written as follows [6].
Frontal cross sectional area of the wheel (for each flow):

$$A_w = \left(\frac{\alpha}{100}\right)\left(\frac{\pi\, d_w^2}{4}\right) = \frac{\pi\, d_w^2}{8} \quad (1)$$

Cross section area of the air stream:

$$A_g = \left(\frac{\alpha}{100}\right)(\varphi)\left(\frac{\pi\, d_w^2}{4}\right) = \frac{\varphi\pi\, d_w^2}{8} \quad (2)$$

Cross section area of the matrix:

$$A_m = \left(\frac{\alpha}{100}\right)(1-\varphi)\left(\frac{\pi\, d_w^2}{4}\right) = \frac{(\varphi-1)\pi\, d_w^2}{8} \quad (3)$$

Porosity (φ) of the matrix can be defined as the ratio of the air stream volume (V_g) to the total volume ((V_{tot}), can be written as:

$$\varphi = \frac{V_g}{V_{tot}} = \frac{V_g}{V_g + V_m} \quad (4)$$

The porous matrix is used to increase the heat transfer surface area (A_s). The surface area can be written as:

$$A_s = \frac{(1-\varphi)\pi\, d_w^2\, L_w}{2\, d_f} \quad (5)$$

Hydraulic diameter is define as [7]:

$$d_h = \frac{4\,(void\ volume)}{surface\ area} = \frac{4\,V_g}{A_s} = \frac{4A}{P} \quad (6)$$

Fig.3. represent he channel geometries that tested in the present study with the hydraulic diameter of each channel.

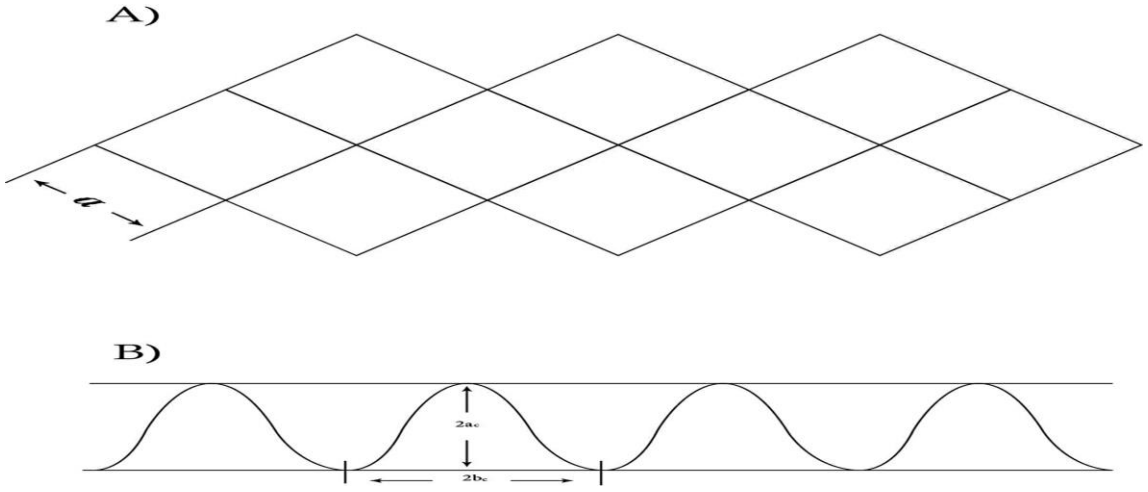

Figure3. Channel geometry where (A) Rhombic and(B) Sinusoidal channel

Where, the hydraulic diameter of rhombic channel can be written as shown below:

$$d_h = \frac{4a^2}{4a} = a \quad (7)$$

While, the hydraulic diameter of sinusoidal channel is shown by the following equations[8].

$$A = 2\ a_c\ b_c \quad (8)$$

$$P \approx 2b_c + 2\sqrt{{b_c}^2 + (a_c\pi)^2}\left(\frac{3+(\frac{2b_c}{a_c\pi})^2}{4+(\frac{2b_c}{a_c\pi})^2}\right) \quad (9)$$

$$d_h = \frac{4A}{P} = \frac{8a_c b_c}{2b_c+2\sqrt{{b_c}^2+(a_c\pi)^2}\left(\frac{3+(\frac{2b_c}{a_c\pi})^2}{4+(\frac{2b_c}{a_c\pi})^2}\right)} \quad (10)$$

To obtain the convective heat transfer coefficient of the flow inside channels with various cross section area it can be given by [6].

$$h_{HT} = \frac{Nu\ Kg\ (1-\varphi)}{\varphi\ d_f} \quad (11)$$

Where, the Nusselt number for flow in various cross section channels for porous media of the recovery wheel is given by the following equation:

$$\text{Nu}= 2+ (0.4\ Re^{\frac{1}{2}} +0.2\ Re^{\frac{2}{3}})Pr^{0.4} \quad (12)$$

The Reynolds number and Prandtl number can be defined by the following relations:

$$\text{Re}= \frac{\rho_g\ u_g\ d_h}{\mu_g} \quad (13)$$

$$\text{Pr}= \frac{\mu_g\ Cp_g}{Kg} \quad (14)$$

The design parameter of the recovery wheel that govern the heat transfer is the number of transfer unit for the heat transfer between the matrix and air (NTU_{HT}) can be defined as shown below:

$$NTU_{HT} = \frac{h_{HT}\ As}{\dot{m}_g\ Cp_g} \quad (15)$$

2.2 Assumption

The model assumes in the present study that**:**

1- The matrix is suppose to be a homogenous porous solid with constant physical properties.

2- A mixing does not take place between the two fluid streams.

3- The thermodynamic properties of the matrix and air are not affected by the small pressure drop.
4- The temperature radial gradient for the air and the matrix is neglected.
5- The heat transfer coefficient is assumed to be constant and not vary with time.

2.3 Governing Equations

The energy equation is applied on an unit volume element of the matrix and the air to derive the governing equation as shown in Fig.4.

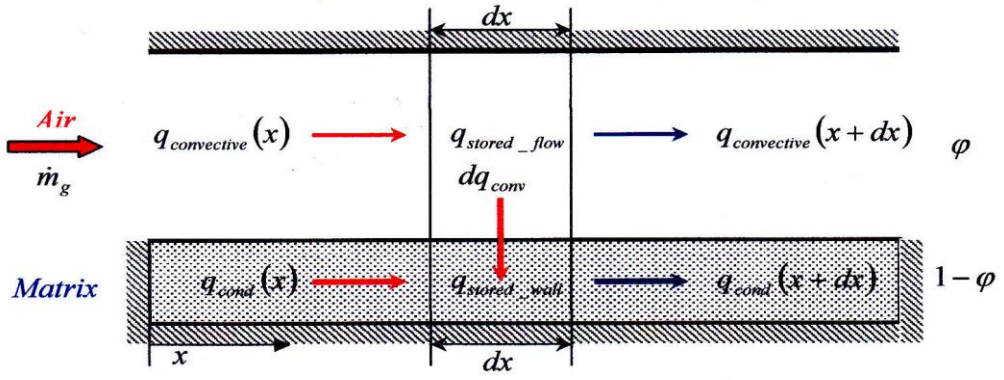

Figure4. The energy balance of the sensible heat wheel.

In the flow region:

By applying the first low of thermodynamic to the unit volume element of the air in the wheel, the energy balance of the flow become [1].

$$q_{stored,flow} = q_{convective}(x) - q_{convective}(x+dx) - dq_{conv} \quad (16)$$

Where:

$$q_{convective}(x + dx) = q_{convective}(x) + \frac{\partial q_{convective}}{\partial x} dx \quad (17)$$

Substituting Eq. (3-17) in Eq. (3-16) gives :

$$q_{stored,flow} = q_{convective}(x) - \left(q_{convective}(x) + \frac{\partial q_{convective}}{\partial x} dx \right) - dq_{conv} \quad (18)$$

$q_{stored,flow}$, dq_{conv} , and $q_{convective}$ can be expressed by the following equations:

$$q_{stored,flow} = \rho_g A_g dx C p_g \frac{\partial T_g}{\partial t} \quad (19)$$

$$dq_{conv} = h_{HT} A_s \frac{dx}{L} (T_g - T_m) \quad (20)$$

$q_{convective}$= ṁC$p_g T_g$ = $U_g A_g \rho_g$C$p_g T_g$ (21)

Substituting Eqs. (3-19), (3-20), and (3-21) in Eq. (3-18) gives:

$\rho_g A_g$dx C$p_g \frac{\partial T_g}{\partial t}$ = $U_g A_g \rho_g$C$p_g T_g$- $U_g A_g \rho_g$Cp_g (T_g+$\frac{\partial T_g}{\partial x}$ dx)- h_{HT} A_s $\frac{dx}{L}$ (T_g-T_m) (22)

It can be simplification to yields: (23)
Eq. (3-23) refers to the temperature distribution of the air in the sensible heat wheel.

$$\varphi \rho_g Cp_g \frac{\partial T_g}{\partial t} = -\varphi U_g \rho_g Cp_g \left(\frac{\partial T_g}{\partial x}\right) - h_{HT} A_v \left(T_g - T_m\right) \quad (23)$$

In the matrix:

By applied the first low of thermodynamic on the unit element in the matrix of the wheel, the energy balance becomes[1].

$$q_{stored\_matrix} = q_{cond}(x) - q_{cond}(x + dx) + dq_{conv} \quad (24)$$

And

$$q_{cond}(x + dx) = \left(q_{cond}(x) + \frac{\partial q_{cond}}{\partial x}\, dx\right) \quad (25)$$

Substituting Eq. (3-25) in Eq. (3-24) gives:

$$q_{stored,matrix} = q_{cond}(x) - \left(q_{cond}(x) + \frac{\partial q_{cond}}{\partial x}\, dx\right) + dq_{conv} \quad (26)$$

Where ($q_{stored,matrix}$ and $q_{cond}(x)$) can be written as follows:

$$q_{stored,matrix} = \rho_m A_m Cp_m\, dx\, \frac{\partial T_m}{\partial t} \quad (27)$$

$$q_{cond}(x) = -K_m A_m \frac{\partial T_m}{\partial x} \quad (28)$$

Substituting Eqs. (3-20), (3-27), and (3-28) in Eq. (3-26) gives:

$$\rho_m A_m Cp_m\, dx\, \frac{\partial T_m}{\partial t} = -K_m A_m \frac{\partial T_m}{\partial x} - K_m A_m \left(-\frac{\partial T_m}{\partial x} - \frac{\partial^2 T_m}{\partial x^2} dx\right) + h_{HT} A_s \left(\frac{dx}{L}\right) \left(T_g - T_m\right) \quad (29)$$

Simplify the above equation for the following equations.

$$(1 - \varphi)\rho_m Cp_m \frac{\partial T_m}{\partial t} = (1 - \varphi) K_m \left(-\frac{\partial^2 T_m}{\partial x^2}\right) + h_{HT} A_v \left(T_g - T_m\right) \quad (30)$$

Eq. (3-30) refers to the temperature distribution of the matrix of the wheel. The initial and boundary conditions that used to complete the solution process as shown in the following[9].

Initial conditions:

The initial conditions that common applied in the solution process are:

$T_g(x,0) = T_{g-o}$, and $T_m(x,0) = \frac{T_{g-s,i}+T_{g-e,i}}{2}$

Boundary conditions:
Supply side: $T_g(x=0,t) = T_{g-s,i}$
Exhaust side: $T_g(x=0,t) = T_{g-e,i}$

For the matrix the boundary condition written mathematically as shown bellow (chosen to be adiabatic):

$$\frac{\partial T_m(x=0,t)}{\partial x} = \frac{\partial T_m(x=L_w,t)}{\partial x} = 0 \quad (31)$$

2.4 *Representation in Dimensionless Form*

The solving of equations (23) and (30) give the temperature distribution of the air and matrix in the recovery wheel. The analyzing and solution become very easy and intelligible when the differential equations turn into dimensionless. The parameters and variables that will turn into dimensionless are:

$t^+ = \frac{t}{\tau}$ Time

$x^+ = \frac{x}{L_w}$ Length

$T_g^+ = \frac{T_g - T_{g-s,i}}{T_{g-e,i} - T_{g-s,i}}$ Temperature of gas

$T_m^+ = \frac{T_m - T_{g-s,i}}{T_{g-e,i} - T_{g-s,i}}$ Temperature of matrix

By using all of the above dimensionless parameter, the partial differential equations (23) and (30) become in the dimensionless form as shown below:

$$\frac{1}{\Gamma}\frac{\partial T_g^+}{\partial t^+} + \frac{\partial T_g^+}{\partial x^+} + NTU_{HT}(T_g^+ - T_m^+) = 0 \quad (32)$$

$$\frac{\partial T_m^+}{\partial t^+} - Fo_m \frac{\partial^2 T_m^+}{\partial x^{+2}} - \frac{NTU_{HT}}{C_r^+}(T_g^+ - T_m^+) = 0 \quad (33)$$

Where C_r^+ is the heat capacity rate ratio of the recovery wheel and defined in the following equation :

$$C_r^+ = \frac{C_r}{C_g} = \frac{(\rho A L Cp)_m \Omega}{(\rho A u Cp)_g} = \frac{(MCp)_m \Omega}{(\dot{m}Cp)_g} \quad (34)$$

The initial and boundary conditions should be also converted to the dimensionless form in order to solve the dimensionless differential equations.

Initial conditions:

For the air: $T_g^+(x^+,0) = T_{g-o}^+$

For the matrix: $T_m^+(x^+,0) = \frac{T_{g-s,i}^+ + T_{g-e,i}^+}{2}$

Boundary conditions:

For the air: $T_{g-s}^+(x^+=0,t^+)=0$, and $T_{g-e}^+(x^+=0,t^+)=1$

For the matrix: $\frac{\partial T_m^+(x^+=0,t^+)}{\partial x^+}=0$, and $\frac{\partial T_m^+(x^+=1,t^+)}{\partial x^+}=0$

2.5 Numerical Model

Equations (32) and (33) can be solved numerically by using the finite difference method. In this study the backward difference and fully-explicit discretization in time was applied to both air and matrix. The solution of the governing equations give the temperature distribution of air and matrix in the sensible heat wheel.

$$\frac{1}{\Gamma}\frac{T_{g\,i}^{+\,n+1}-T_{g\,i}^{+\,n}}{\Delta t^+}+\frac{T_{g\,i}^{+\,n}-T_{g\,i-1}^{+\,n}}{\Delta x^+}+NTU_{HT}\left(T_{g\,i}^{+\,n}-T_{m\,i}^{+\,n}\right)=0 \quad \text{for air} \tag{35}$$

$$\frac{T_{m_i}^{+\,n+1}-T_{m_i}^{+\,n}}{\Delta t^+}-\frac{Fo_m}{\Delta x^{+\,2}}\left(T_{m\,i-1}^{+\,n}-2T_{m_i}^{+\,n}+T_{m\,i+1}^{+\,n}\right)-\frac{NTU_{HT}}{Cr^+}\left(T_{g\,i}^{+\,n}-T_{m\,i}^{+\,n}\right)=0 \quad \text{for matrix} \tag{36}$$

Equations (35) and (36) can be used for both supply side and exhaust side. To avoid the negative fluctuation term in the above equations, the change in dimensionless time is derived from the finite difference equations of air and matrix as following:

$$\frac{1}{\left(\frac{\Gamma}{\Delta x^+}+\Gamma NTU_{HT}\right)} \geq \Delta t^+ \quad \text{in air}$$

$$\frac{1}{\left(2\frac{Fo_m}{\Delta x^{+\,2}}+\frac{NTU_{HT}}{Cr^+}\right)} \geq \Delta t^+ \quad \text{in matrix}$$

Finally, the sensible effectiveness of recovery wheel can be calculated according to Eq. (37)[10].

$$\varepsilon_s = \frac{c_2(T_1-T_2)}{c_{min}(T_1-T_3)} \tag{37}$$

After offer all the main governing equations and finite difference equation, the average outlet temperature of the supply and exhaust period should be calculated from these equations in order to estimate the sensible effectiveness of the wheel. Computer program

built in MATLAB (version 7.6 R2008a) to solve the finite difference equations, and find the effectiveness of the recovery wheel.

3. Experimental Work

To accomplish experimental investigation, the test rig is designed and manufactured as described and photographed in figure (5). The test rig consists of (test room, air conditioning, two centrifugal fans, motor, case and recovery wheel, four ducts, and measurement devices).

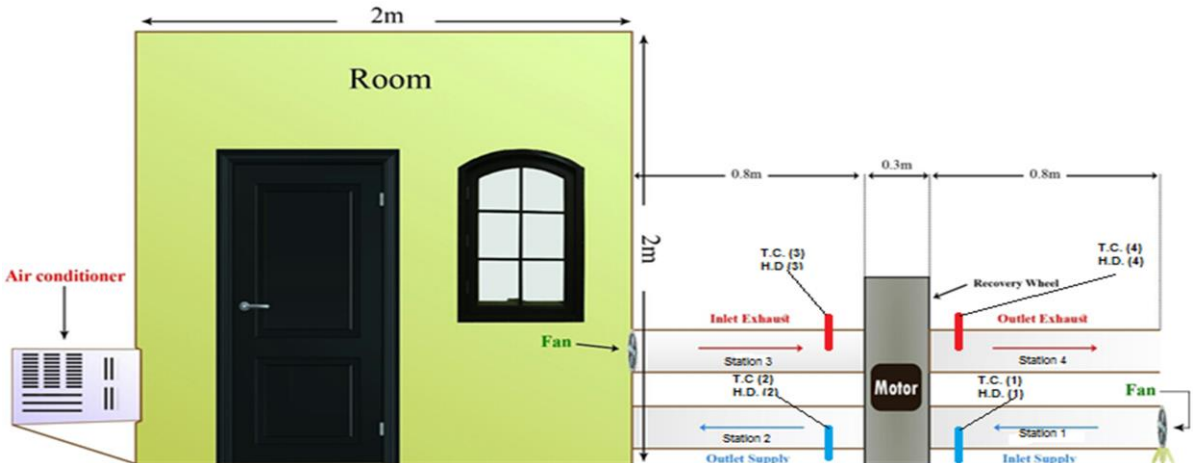

Figure5. Description of the test rig.

The test room was made of sandwich panel with dimension $(2m \times 2m \times 2m)$. A window type air-conditioning (gives heating and cooling loads) was used to obtain the temperature and relative humidity recommended in air-conditioned places according to the Iraqi Mechanical Ventilation Code [11]. The tests of this study was conducted in winter where the range of temperature and relative humidity required in room was (21 ± 2 ℃ and $50\pm10\%$) respectively, while the temperature and relative humidity in surrounding was (14 ± 3℃ and $50\pm10\%$) respectively. Two shapes of aluminum channels geometry were used (rhombic and sinusoidal channels). The hydraulic diameter of rhombic and sinusoidal channel was (10 and 7.9 mm) respectively. The effect of both speed and wheel thickness on the sensible effectiveness were studied. three wheels of diameter 600mm and thickness (50, 100, and 150mm) has been manufactured for each channel geometry, while the speed used in this study was (5, 10, 15, 20, 25 rpm), and the volume flow rate was (150 CMH)[12].

4. Results and Discussion

The experimental effectiveness results of recovery wheel shows in Fig.6, while Fig.7. was show numerical results for rhombic and sinusoidal channels respectively. The effect of both speed and wheel thickness on the sensible effectiveness for rhombic and sinusoidal channels shows Fig.6. respectively. It is seen from these figures that, the effectiveness for

rhombic and sinusoidal channels was increased with increasing wheel speed because the average temperature of the matrix becomes close to the air when the sensible heat wheel rotates slowly and this will decrease the heat transfer as the temperature difference becomes limited, while the amount of trapped air in the channel of the wheel increases when the wheel rotates fast and this increases the heat transfer between the matrix and air which lead to increase the effectiveness. In this study, the optimal wheel revolution speed was (25 rpm) at each value of volume flow rate and length of wheel for two channels. The effectiveness of recovery wheel is also affected by the wheel thickness as shown in Fig.6. It can be concluded from these figures, the increase of wheel thickness will increase the sensible effectiveness due to increase the area of heat transfer and this will increase the time of exchange the energy between the supply and exhaust air streams. When the wheel thickness increased from (50 to 150 mm), the effectiveness will be increase from (74. 39 to 81.48 %) for rhombic, and (79.16 to 85.89 %) for sinusoidal channel at speed (25 rpm). The sensible effectiveness for the sinusoidal channel is higher than the rhombic channel at any wheel speed and wheel thickness because the rhombic channel has the highest hydraulic diameter, and therefore this leads to a lower heat transfer coefficient and heat transfer area. When the volume flow rate and wheel speed were (150 CMH and 25 RPM) respectively for each length (50, 100, and 150 mm), the experimental sensible effectiveness of rhombic channel was (74.39, 78.26, and 81.48 %), while the effectiveness of sinusoidal channel was (79.16, 8v 2.82, and 85.89 %) at rates increase (1.06, 1.058, and 1.054 time) respectively. Finally can be seen from Fig.6 and Fig.7 that, there is a convergence between the results of experimental and numerical effectiveness with maximum error reached to (23.27%) while, the minimum error (2.42%). The main reason for this error was the leakage between the wheel and outlet, and between the supply and exhaust air streams.

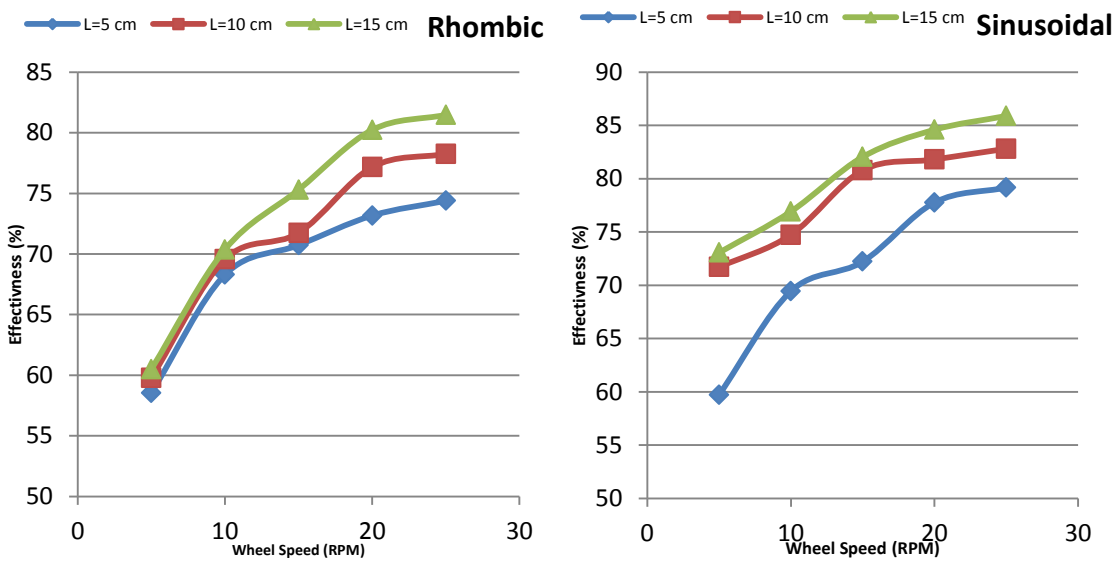

Figure 6. Experimental results of the effectiveness at each length for rhombic and sinusoidal channels.

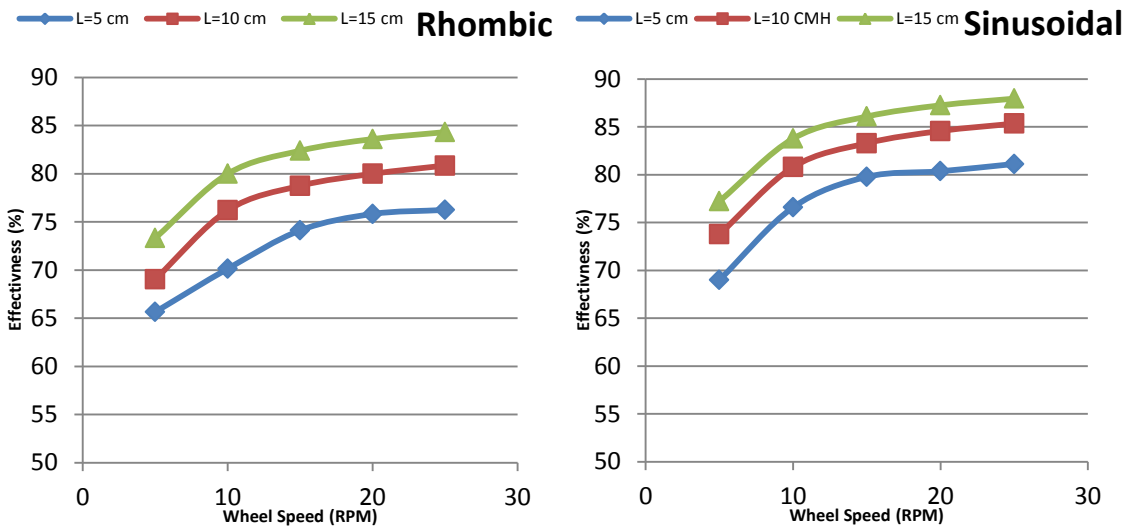

Figure7. Numerical results of the effectiveness at each length for rhombic and sinusoidal channels.

Abbreviations

Symbols	Definition	Units
A	Cross section area	m^2
A_w	Frontal cross section area of the half split wheel	m^2
A_g	Cross section area of the air stream	m^2
A_m	Cross section area of matrix	m^2
A_s	Convective heat transfer surface area	m^2
A_v	Geometrical surface to volume ratio	m^2/m^3
d_w	Diameter of wheel	m
d_f	Diameter of fiber	m
d_h	Hydraulic diameter	m
h_{HT}	Convective heat transfer coefficient	$W/m^2.K$
i	Index of stepping along x-direction	
k_g	Thermal conductivity of gas	$W/m.K$
k_m	Thermal conductivity of matrix	$W/m.K$
L_w	Length of wheel	m
$\dot{m}_g$	Mass flow rate of gas	kg/s
NTU_{HT}	Number of heat transfer unit	
Nu	Nusselt number	
Pr	Prandtl number	
Re	Reynolds number	
T_g	Temperature of gas	K
T_g^+	Dimensionless temperature of gas	
T_m	Temperature of matrix	K
T_m^+	Dimensionless temperature of matrix	
t	Time	s
t^+	Dimensionless time	
U_g	Mean gas velocity	m/s
V_{tot}	Total volume of half split wheel	m^3

V_m	Volume of matrix	m^3
V_g	Volume of air	m^3
x	Axial coordinate	m
x^+	Dimensionless length	

5. Conclusions

1. The sensible effectiveness of recovery wheel will increase with increasing the speed and wheel thickness.
2. the sensible effectiveness and of sinusoidal channel are higher than rhombic channel.
3. There is a satisfactory match could be seen between the numerical and experimental results.

7. References

1. Abdulmajeed S. Al-Ghamdi. (2006). *"Analysis of Air-to-Air Rotary Energy Wheels"* Ph.D Thesis, University of Ohio.
2. American Society of Heating, Refrigeration and Air Conditioning Engineers(2001). *"ASHRAE, Handbook of Fundamentals"* New York.
3. S. Delfani, G. Heidarinejad, H. Pasdar Shahri .(2009*)." The Effect of Geometrical Characteristics of Desiccant Wheel on Its Performance"* IJE Transactions B: Applications, Vol. 22, No. 1, pp. 63-75.
4. Monali S. Bhojane, M.S. Deshmukh (2010*)." Effect of Air Preheating on Performance of C.I. Engine Using Energy Wheel"* Third International Conference on Emerging Trends in Engineering and Technology, pp. 686-690.
5. Manu Prakash, Shrikant Arora, S.N.Mishra (2012). *"QUALITY IMPROVEMENT OF INDOOR AIR BY USING HEAT RECOVERY WHEEL"* International Journal of Research in Engineering and Technology, Vol. 1, Issue.4, pp. 526-531.
6. Dullien, F. A. L. (1992). *"Porous Media: Fluid Transport and Pore Structure"* Academic Press, San Diego.
7. Kaviany (2002). *"Principles of Heat Transfer"* John Wiley & New York.
8. Avadhesh Yadav, Laxmikant Yadav (2014). *" Comparative Performance of Desiccant Wheel with Effect and Ordinary Regenerative Sector Using Mathematical Model"* Journal of Heat Mass Transfer, pp.1465-1478.
9. Duram, and Alam (2002). Joint Thermophysics and Heat Transfer Conference, St. Louis, Missouri,.
10. American Society of Heating, Refrigerating, and Air-Conditioning (2008). *" Method of Testing Air-to-Air Heat/Energy Exchangers"* Standard 84.
11. "Iraqi blog of mechanical ventilation" 2013.
12. Duaa J. Mohamed."*Experimental and Numerical Study for the Performance of Recovery Wheel".*Ms.c. Thesis, Al-Mustansiriyah University, Faculty of Engineering, Mechanical Engineering Department, 2016.